



Schweizerische Eidgenossenschaft
Confédération suisse
Confederazione Svizzera
Confederaziun svizra

Eidgenössisches Departement für Umwelt, Verkehr, Energie und
Kommunikation UVEK

Bundesamt für Energie BFE

Jahresbericht 15. November 2011

Cost-efficient and reliable thermoelectric converters for industrial waste heat recovery TECIND

Auftraggeber:

Bundesamt für Energie BFE
Forschungsprogramm Elektrizitätstechnologien und -anwendungen
CH-3003 Bern
www.bfe.admin.ch

Kofinanzierung:

EMPA, CH-8600 Dübendorf
vonRoll casting (emmenbrücke) ag, CH-6020 Emmenbrücke

Auftragnehmer:

EMPA Dübendorf
Überlandstrasse 129
CH-8600 Dübendorf
www.empa.ch

Autoren:

Gesine Saucke, EMPA, gesine.saucke@empa.ch
David Moser, EMPA, david.moser@empa.ch
Anke Weidenkaff, EMPA, anke.weidenkaff@empa.ch

BFE-Bereichsleiter: Dr. Michael Moser
BFE-Programmleiter: Roland Brüniger
BFE-Vertragsnummer: SI / 500601-01

Für den Inhalt und die Schlussfolgerungen sind ausschliesslich die Autoren dieses Berichts verantwortlich.

Zusammenfassung

Ein Ansatz für den Ressourcen-sparenden Umgang mit Energie ist die Nutzung von Abwärme mit Hilfe von thermoelektrischen Generatoren, die Wärme direkt in elektrische Energie umwandeln. Im Gegensatz zu anderen entropischen Konversionstechniken zeichnen sich thermoelektrische Module durch hohe Verlässlichkeit und geringen Wartungsaufwand aus, da sie keine beweglichen Teile besitzen. Das Ziel dieses Projektes ist die Entwicklung und Herstellung optimierter, thermoelektrischer Module für die Abwärmenutzung von industriellen Hochtemperatur-Prozessen, um einen Beitrag zu einer nachhaltigen Energiewirtschaft zu leisten.

Ein profitabler Betrieb thermoelektrischer Generatoren erfordert die Kenntnis der thermischen Randbedingungen. Erste Ergebnisse bezüglich der lateralen Temperaturverteilung auf dem Deckel des Giesserei-Ofens werden dargestellt. Da sich die Randbedingungen mit der Zeit ändern, wurden die Temperaturen über einen kompletten Produktionszyklus aufgenommen. Zusätzlich sind Wärmeflussmessungen geplant, um die Module zu optimieren und die generierbare elektrische Leistung abschätzen zu können.

Um die Effizienz von Konvertern zu maximieren, müssen die Materialien passend zu den Randbedingungen ausgewählt werden. Generell sind die verwendeten Isolationsmaterialien der Hochtemperaturprozesse der Giesserei in Emmenbrücke Keramiken. Aus diesem Grunde sollen auch für die Konverter ähnliche Materialien eingesetzt werden.

Unter den keramischen Oxiden konnten besonders vielversprechende, thermoelektrische Materialien identifiziert werden, da sie hochtemperaturstabil, ungiftig und günstig zu produzieren sind. Zunächst wurden angepasste, geschichtete Cobaltoxide synthetisiert, welche sich im Vergleich zu anderen Oxiden durch einen besonders hohen Power-Faktor und eine hohes ZT auszeichnen. Für Bi-substituiertes $\text{Ca}_{3-x}\text{Bi}_x\text{Co}_4\text{O}_{9+\delta}$, wurde insbesondere der Einfluss des Sauerstoffgehaltes auf die thermoelektrischen Eigenschaften untersucht. Aus der Untersuchung geht hervor, dass ZT durch die Kontrolle des Bismuth- und Sauerstoffgehaltes von 0.12 auf 0.19 erhöht werden kann. Des Weiteren verdeutlichen unsere Ergebnisse den starken Einfluss des Sauerstoffgehaltes, der in oxidischen Systemen nicht vernachlässigbar ist.

Abstract

One approach to a resource-conserving use of energy is the recovery of waste heat with thermoelectric devices, which directly convert heat into high-quality electrical energy. In contrast to other heat conversion techniques, thermoelectric modules are characterized by high reliability and low maintenance as no moving parts are involved. The aim of this project is to develop and manufacture optimized thermoelectric modules for waste heat recovery from industrial production processes in order to make a contribution to a sustainable usage of energy.

A profitable operation of thermoelectric converters requires the knowledge of the temperature boundary conditions. First results concerning the lateral temperature distribution on the top cover of a melting furnace are presented. Since the boundary conditions are varying with time, temperatures were measured over a whole production cycle. In addition, heat flow measurements are planned in order to be able to optimize the modules and to estimate the electrical generator power.

To maximize the converter efficiency, the thermoelectric materials have to be chosen according to the boundary conditions. Oxides are particularly promising thermoelectric materials because they are chemically stable at elevated temperatures, non-toxic and produced at low cost. First, misfit-layered cobalt oxides, which provide an exceptionally high power factor and a high ZT compared to other oxides, were synthesized. Using Bi-substituted $\text{Ca}_{3-x}\text{Bi}_x\text{Co}_4\text{O}_{9+\delta}$, the influence of the oxygen content on the thermoelectric properties was studied in particular. The measurements reveal that the ZT can be increased from 0.12 to 0.19 by controlling the Bi and the oxygen content. Furthermore, our results demonstrate the strong influence of the oxygen content, which cannot be neglected in oxide systems.

Introduction

Due to the limited fossil fuel resources, the promotion of renewable energies becomes more and more important. Additionally, efforts have to be made to conserve resources in general. One way in this regard is the thermoelectric recovery of waste heat arising from many industrial production processes. The efficient application of thermoelectric modules requires a design in consideration of the boundary conditions, which are defined by the temperature and the heat flux. In this project, modules will be designed to convert the waste heat at the top of a commercial melting furnace. As the boundary conditions strongly depend on the production process, the time-dependence of temperature and heat flux have to be analyzed carefully.

Based on the analysis of the operating parameters, thermoelectric materials with maximal efficiency in this temperature region have to be chosen. Especially, due to the time variable boundary conditions materials with good efficiencies in a broad temperature range are needed.

Oxide materials are promising candidates for thermoelectric applications as they are chemically stable at high temperatures and their properties can be tuned easily by elemental substitution (see results from preceding projects¹⁻³ [Weidenkaff, A., Robert, R., Aguirre, M.H., Bocher, L., Lippert, T., S. Canulescu, Development of Thermoelectric Oxides for Renewable Energy Conversion Technologies, *Renewable Energy*, 33 (2008) 342-347, Robert, R. Aguirre, M. H., Hug, P., Reller, A. and Weidenkaff, A., High temperature thermoelectric properties of Ln(Co, Ni)O₃ (Ln = La, Pr, Nd, Sm, Gd, and Dy) compounds, *Acta Materialia*, **55** (2007) 4965-4972, Bocher L., Aguirre M.H., Robert R., Logvinovich D., Bakardjieva S., Hejtmanek J. and Weidenkaff, A., High-temperature stability, structure and thermoelectric properties of CaMn_{1-x}Nb_xO₃ phases, *Acta Mat.* **57** (2009) 5667-5680..] Furthermore, they are inert and therefore environmentally friendly and manufacturing costs are low. An interesting group of oxides are misfit-layered cobaltates as they provide exceptionally high power factors $P=S^2\sigma$ due to a relatively high Seebeck coefficient S combined with a high electrical conductivity σ .

These, at first glance, contradictory characteristics originate from their peculiar crystal structure. Misfit oxides are composed of two interpenetrating subsystems where the ratio of their periodicities is a non-integer number. This lattice misfit also leads to a low thermal conductivity perpendicular to the planes of the subsystems. As a first step, Bi was substituted for Ca in the misfit oxide Ca₃Co₄O₉ aiming to further reduce the thermal conductivity. The thermoelectric properties were analyzed and the oxygen contents were measured, as the latter may severely alter the properties of oxide materials⁴⁻⁵ [Weidenkaff, A., Aguirre, M., Bocher, L., Trottmann, M., Tomes, P., and Robert, R., Development of perovskite-type cobaltates and manganates for thermoelectric oxide modules, *J. Korean Cer. Soc.*, **47**, (2010) 47-53., Moser, D., Karvonen, L., Populoh, S., Trottmann, M., Weidenkaff, A., Influence of the Oxygen Content on Thermoelectric Properties of Ca_{3-x}Bi_xCo₄O_{9+δ} System, *J. Solid State Sciences*, in press, 10.1016/j.solidstatesciences.2011.10.001.].

Theory and state of the art

Thermoelectric modules

Fig. 1 shows a simple thermoelectric converter consisting of a p- and an n-conducting semiconductor leg connected by an electrically conducting material. If a temperature gradient is applied to the legs electrons and holes in the n- and p- legs, respectively, diffuse from the hot to the cold side. Since the legs are connected electrically in series, an electric current I is generated under load.

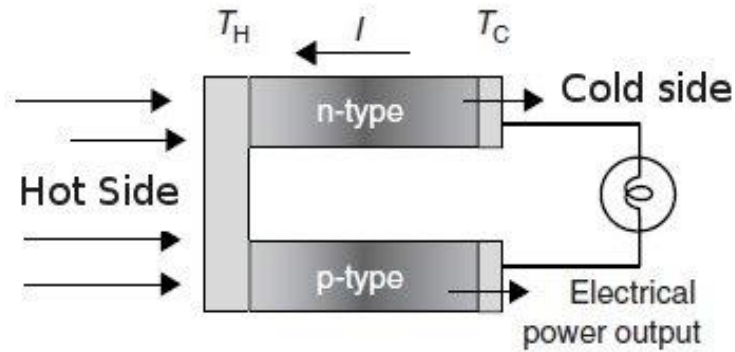


Figure 1: Scheme of a thermoelectric converter consisting of a p-type and n-type semiconductor.¹

The efficiency of a module is determined by the averaged thermal conductivity κ_{np} of the p-type and n-type leg and the module's overall electrical resistance R . It is defined² as the quotient of the electric power output P and the thermal energy supplied at the hot side Q

$$(1.21) \quad \eta = \frac{P}{Q} = \frac{I^2 R}{\kappa_{np}(T_H - T_C) - \frac{1}{2} I^2 R}$$

The maximum efficiency is given by

$$(1.22) \quad \eta_{\max} = \frac{T_H - T_C}{T_H} \cdot \frac{\sqrt{1 + Z_C \bar{T}} - 1}{\sqrt{1 + Z_C \bar{T}} + T_C / T_H}, \quad \bar{T} = \frac{T_H + T_C}{2}$$

where Z_C is the mean Figure of Merit of the whole module. The equation reveals that the maximum efficiency is limited by the Carnot efficiency

$$\eta_c = \frac{T_H - T_C}{T_H}$$

An improvement of the conversion efficiency of a thermoelectric module can be attained by either increasing the Figure of Merit Z or the temperature difference $\Delta T = T_H - T_C$ (Fig.2).

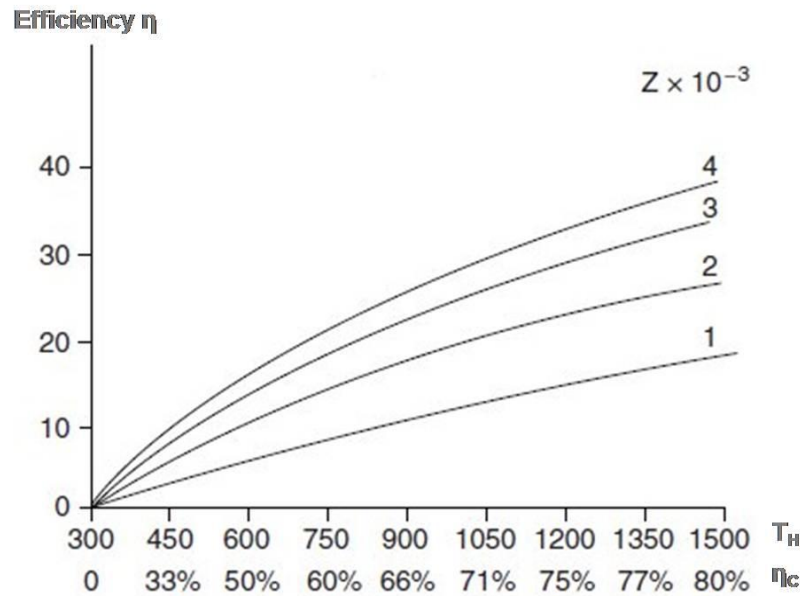


Figure 2. Efficiency η of a thermoelectric module as a function of the temperature at the hot side T_H while the temperature at the cold side is constant ($T_C = 300$ K). The corresponding Carnot efficiency η_C is stated below the x-axis. The module efficiency increases with increasing Figure of Merit Z .^{6,7}

Thermoelectric Materials

Based on a comprehensive literature survey Fig. 3 shows the currently most common thermoelectric materials for different temperature ranges. The maximum ZT values are around one corresponding to an efficiency of 3-8%. However, the downside of all of these semiconducting materials is that they are rare, toxic, expensive or unstable at elevated temperatures.

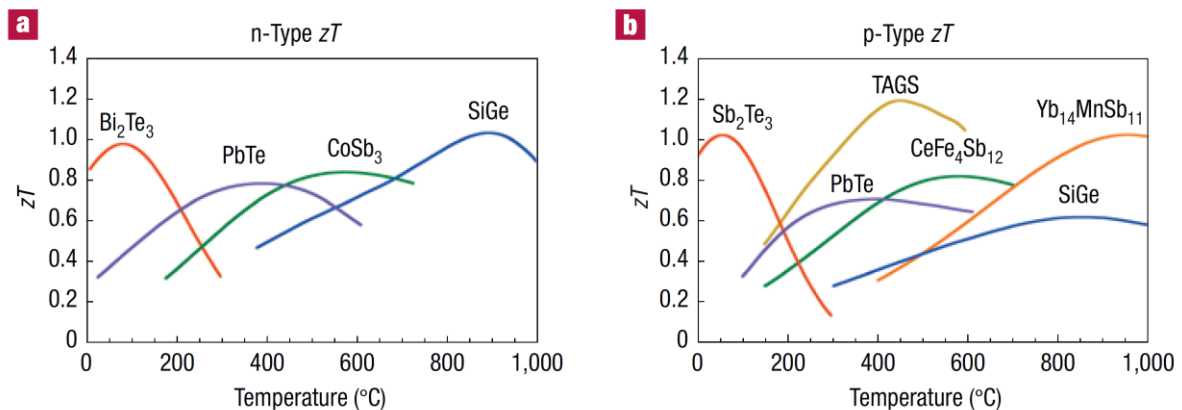


Fig. 3: Figure of Merit ZT of conventional a) n-type and b) p-conducting thermoelectric materials.⁸

As the efficiency increases with increasing temperature difference along the thermocouple, thermoelectric materials with a good chemical stability at high temperatures are needed.

In general, oxide materials provide this stability as they are already oxidized. Therefore, they can be operated in air instead of an inert atmosphere. In addition, they are nontoxic and can be synthesized at low cost. However, the currently achievable ZT values still fall short of those of the materials presented in Fig. 3. But yet they have a high potential to enhance the thermoelectric efficiency as their properties can be easily tuned by cationic substitution.

Basically, there are three concepts to improve the thermoelectric properties of oxide materials:

- Nano-structuring to reduce the phonon part of the thermal conductivity
- Cationic substitution to improve the electrical conductivity owing to charge carrier doping or to reduce the thermal conductivity due to an increase of the lattice disorder
- Variation of the oxygen content to change the charge carrier densities and therefore the electrical conductivity and the Seebeck coefficient

In this report we focus on misfit-layered cobaltates. They can be described by the general formula, $[M_m A_2 O_{m+2}]_q [CoO_2]$ ($M = Co, Bi, Pb, Tl, \text{etc.}; A = Ca, Sr, Ba, \text{etc.}; m = 0, 1, 2; q \geq 0.5$), where $[M_m A_2 O_{m+2}]$ stands for the rock-salt-structured (RS) block and $[CoO_2]$ for the hexagonal (H) block, which are stacked alternately and discontinuously forming a loosely bound layered structure. While the number of M -cation layers in the $[M_m A_2 O_{m+2}]$ block is defined by the suffix m , the “misfit parameter” q ($\equiv b_H/b_{RS}$, where b_H and b_{RS} are the mutually incommensurate lattice parameters of the two block types) is a measure of the mismatch between the two blocks. The hexagonal $[CoO_2]$ layer consisting of edge-sharing CoO_6 octahedra is the basic building block present in all misfit-layered cobalt oxides. Due to the misfit-layered structure they exhibit a low thermal conductivity perpendicular to the layers and a good electrical conductivity within the layers.

Experimental work and results

Determination of the boundary conditions

Temperature and heat flux strongly influence the efficiency of thermoelectric modules and have thus to be carefully analyzed. During the week, melting furnaces at vonRoll casting ag (Fig. 4 a) are continuously operated and kept at relatively high temperature using a gas burner during weekends to prevent corrosion of the oven. During the industrial production process metals are molten in the oven, the cast is removed and the oven is refilled periodically leading to varying temperatures and fluxes at the top cover of the furnace.

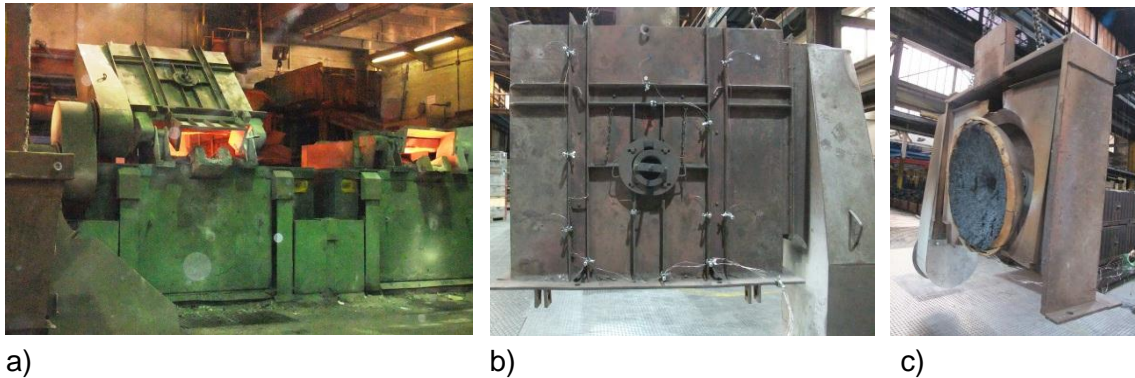


Figure 4: a) Melting furnaces at vonRoll casting
b) Top cover of the furnace with installed thermo couples
c) Bottom side of the top cover of the melting furnace

As a first step, the course of the temperature at the furnace top was measured during a seven days production cycle using eight thermocouples. Temperatures were recorded every 10 seconds and averaged over intervals of 2 minutes. The top of the furnace cover with the thermocouples is shown in Fig. 4 b) and the bottom of the cover in Fig. 4 c).

The infrared images in Fig. 5 provide a more detailed illustration of the temperature conditions at the top of the furnace cover. The image in Fig 5 a) was taken during the melting process while the image in Fig. 5 b) shows the conditions when the oven was not used but kept at elevated temperatures using a gas burner. Measurements are still in progress and complete data will be available soon.

Furthermore, the heat flux will be measured in order to calculate the temperatures T_h and T_c at the hot and the cold side of the module, respectively. Here T_h might differ from the furnace surface temperature, which is mainly determined by radiation and convection. Module installation, however, changes the heat flow as thermal conduction becomes important. Careful modeling of the conditions considering thermal resistances and entropy transport in the modules will be necessary. In addition, the heat flux serves to estimate the output power of the thermoelectric converters.

Moreover, the area available for thermoelectric conversion was determined. The installation of thermoelectric generators appears to be difficult due to the geometrically irregular surface of the furnace cover.

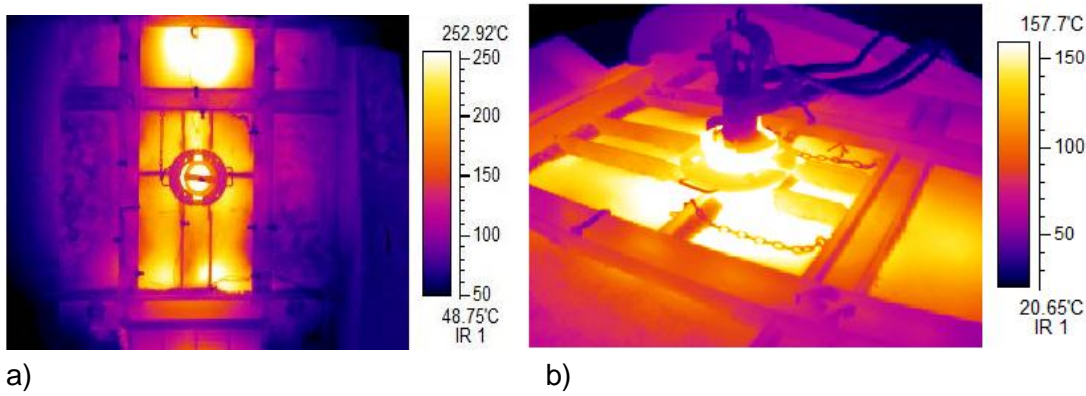


Fig. 5: Infrared image of the top cover of the furnace
 a) during the melting process
 b) during heating with a gasburner

Materials - Synthesis and characterization

Like the related Na_xCoO_2 system⁹, misfit-layered $\text{Ca}_{3-x}\text{Bi}_x\text{Co}_4\text{O}_{9+\delta}$ is known for its exceptionally high power factor $PF = S^2\sigma$, where S is the Seebeck coefficient and σ the electrical conductivity.¹⁰⁻¹³ Therefore, this promising material was chosen to study the tuneability of the thermoelectric properties by Bi and oxygen content variations.

Samples up to substitution levels of $x = 0.2$ were synthesized by a solid state reaction (SSR) method. The precursor powders Co_3O_4 (99.7%), CaCO_3 (99.5%) and Bi_2O_3 (99.5%) were mixed in stoichiometric ratios and calcined at 1173 K in air for 33 h with one intermittent grinding and pelletizing at an uniaxial pressure of 194 MPa. The phase-pure products were reground and uniaxially hot-pressed at 973 K and 66 MPa for 2h under nitrogen resulting in pellets with $88\% \pm 5\%$ of the theoretical density. The pellets were cut in bars and post-annealed in air and argon, respectively.

X-ray diffraction (XRD) analysis proves phase purity and further reveals a variation of the lattice parameter due to the Bi doping, while the layer misfit parameter q remains constant.

A scanning electron microscopy (SEM) image of the microstructure is shown in Fig. 6. The crystallite size of the Bi containing samples seems to be smaller compared to the unsubstituted sample. However, as the crystallite size is still far above nanoscale it is not limiting the mean free path of the electrons and thus not severely affecting the thermoelectric properties.

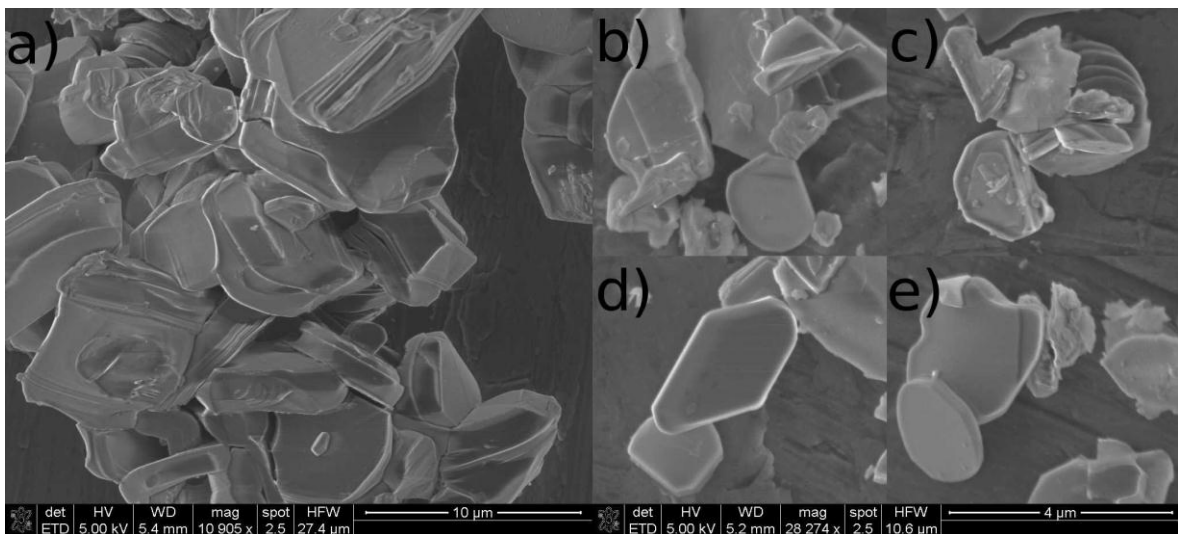


Figure 6: SEM images of (a) $\text{Ca}_3\text{Co}_4\text{O}_{9+\delta}$ and (b)(c)(d)(e) $\text{Ca}_{2.8}\text{Bi}_{0.2}\text{Co}_4\text{O}_{9+\delta}$ synthesized by SSR. The right scale applies to the images (a) to (e).

The oxygen content of the samples was measured by thermogravimetric analysis (TGA). The oxygen non-stoichiometry parameter δ of air-annealed samples does not display a clear dependency on x , while Ar-annealed samples exhibit a systematic decrease of δ with increasing x (Tab. 1).

x	Prepared in air		Prepared in Ar	
	Weight loss (%)	δ	Weight loss (%)	δ
0.00	19.97	0.30	19.86	0.26
0.05	20.1	0.42	19.54	0.20
0.10	20.04	0.46	19.17	0.12
0.15	19.79	0.43	19.12	0.15
0.20	19.43	0.34	18.65	0.03

Table 1: Weight loss and oxygen non-stoichiometry parameter δ of air- and Ar-annealed $\text{Ca}_3\text{Co}_4\text{O}_{9+\delta}$ measured by reductive TGA

Fig. 7 and 8 show that the Seebeck coefficient of Ar-annealed samples increases at elevated temperatures with increasing Bi substitution while the electrical conductivity decreases. In contrast, no clear dependency is observed for air-annealed samples.

Theoretically, it is expected that the substitution of Bi^{3+} for Ca^{2+} introduces negative charge carriers and therefore reduces the charge carrier density in the p-conducting cobaltate. Accordingly a decrease of the electrical conductivity is expected for higher x irrespective of the post-annealing procedure. As this is not the case, it is evident that the influence of the oxygen content has to be taken into account. The introduction of O^{2-} changes the valence of the Co ions, more precisely the amount of Co^{4+} in the Co^{3+} matrix increases and therefore produces additional holes. Thus, in air-annealed samples the additional oxygen counteracts the effect of Bi^{3+} substitution, while in Ar-annealed samples the effect is enhanced due to the reduction in the oxygen content with increasing x .

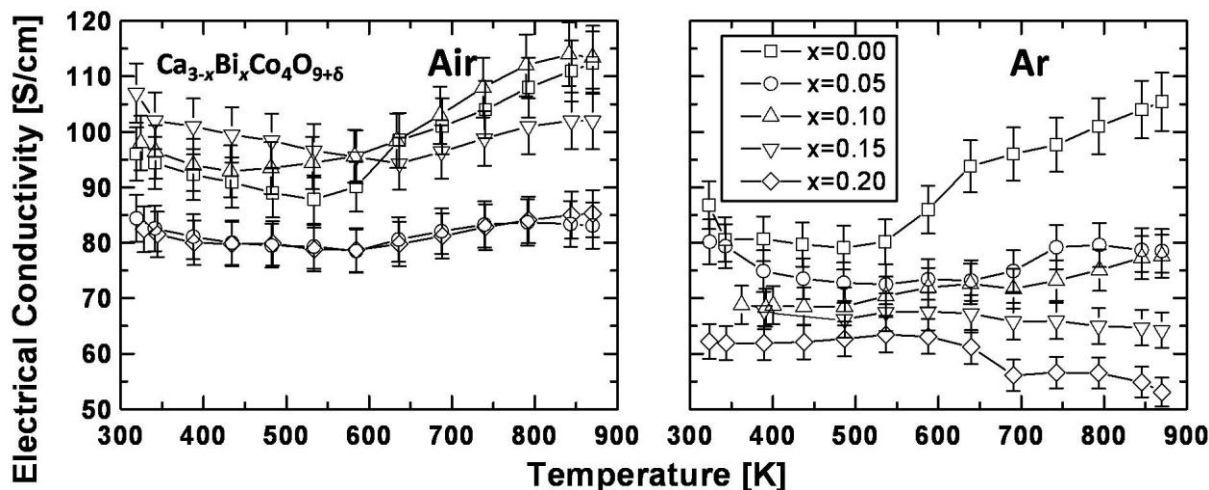


Figure 7: Electrical conductivity of $\text{Ca}_{3-x}\text{Bi}_x\text{Co}_4\text{O}_{9+\delta}$ measured in (a) air and (b) argon atmosphere. A maximum relative error of $\Delta\sigma = \pm 5\%$ was determined by repeated measurements with identical samples.

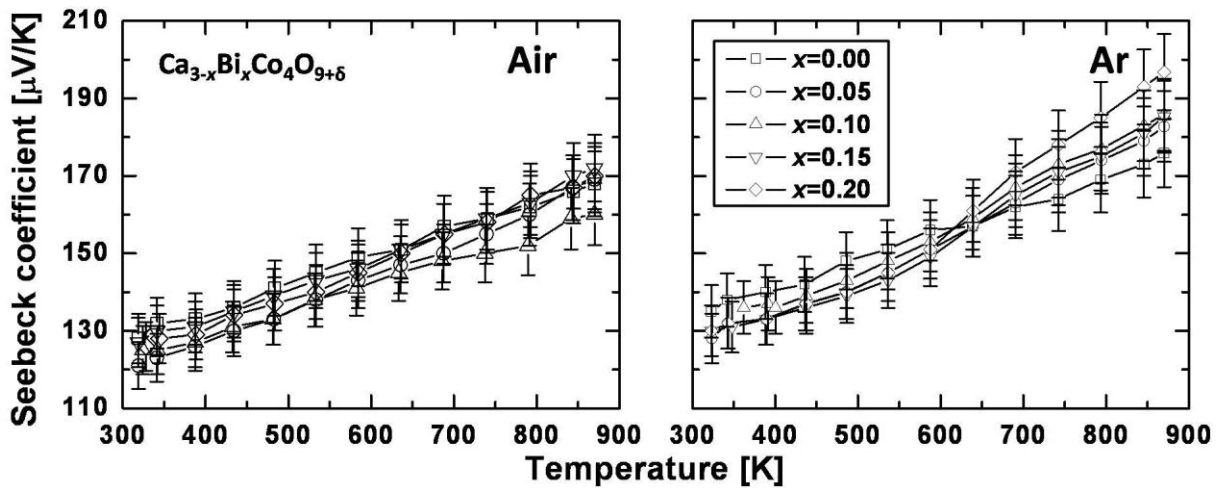


Figure 8: Seebeck coefficient of $\text{Ca}_{3-x}\text{Bi}_x\text{Co}_4\text{O}_{9+\delta}$ measured in air (a) and argon (b) atmospheres. A maximum relative error of $\Delta\sigma = \pm 5\%$ was determined by repeated measurements with identical samples.

In order to sustain electroneutrality, the introduction of Bi^{3+} is accompanied by a reduction of the Co^{4+} concentration with increasing x . According to the theory of Koshibae⁹ this should decrease the spin-entropy part of S . The reduction of S , however, does not occur as the increase in δ , and therefore n , counteracts the charge carrier reduction in air-annealed samples.

In Ar-annealed samples δ and x , and therefore n as well, decrease simultaneously. Interestingly, the trend expected according to the stated theory¹⁴ fails to appear. Instead, an overall increase of S is observed. From this result it can be concluded that the charge-carrier-entropy effect is enhanced, i.e. the remaining holes are provided with additional entropy. This interpretation is supported by the metallic electrical conductivity, which is predicted for the system described by Koshibae.⁹ The increase of S with increasing x is most pronounced at $T > 650$ K.

Furthermore, the thermal conductivity has a great influence on the thermoelectric conversion efficiency. In Fig. 9 the total thermoelectric conductivity $\kappa = c_p \cdot \rho \cdot \alpha$ is shown. The thermal diffusivity (α) was obtained by laser flash absorption (LFA) technique using a Netzsch 457 MicroFlash system, the heat capacity (c_p) was determined by differential scanning calorimetry (DSC) using a Netzsch DSC-404 and the absolute density (ρ) was measured with a pycnometer.

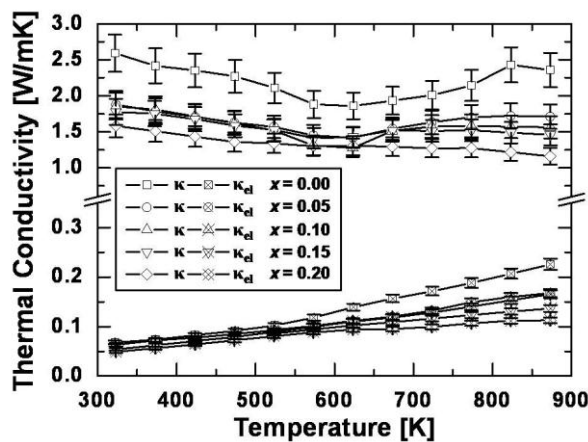


Figure 9: Total (κ) and electronic (κ_{el}) thermal conductivity of $\text{Ca}_{3-x}\text{Bi}_x\text{Co}_4\text{O}_{9+\delta}$ measured in Ar. Maximum relative errors $\Delta\kappa = \pm 10\%$ and $\Delta\kappa_{el} = \pm 5\%$ were determined by repeated measurements with identical samples.

In addition to the total thermal conductivity Fig. 7 also shows the electronic contribution (κ_{el}) to the thermal conductivity, which was estimated using the Wiedemann-Franz law $\kappa_{el} = L_0 \sigma(T) T$ with the Lorenz-number $L_0 = 2.44 \cdot 10^{-8} \text{ V}^2/\text{K}^2$. κ_{el} increases with increasing temperature, compared to the phonon thermal conductivity κ_{ph} . However, it is rather small, which is typical for oxides. The reduction in the total thermal conductivity mainly originates from the reduction in the phononic contribution owing to the introduction of the heavy Bi^{3+} ion. With a substitution level of $x=0.2$ a reduction in κ of about 50% was achieved at 870K.

Finally, the Figure of Merit $ZT = S^2 \cdot \sigma / \kappa$ can be calculated from the data. The calculation was based on the thermal conductivity of Ar-annealed samples. Despite of the decrease of the power factor $S^2 \cdot \sigma$ ZT shows a slight overall enhancement with increasing x (Fig. 10), due to the strong decline of κ . This characteristic is even more pronounced for air-annealed samples, because the decrease in electrical conductivity with increasing x is lower than for Ar-annealed samples. The lowest $ZT_{870\text{K}} = 0.12$ was obtained with $x = 0.00$ showing no significant difference between the two atmospheres, whereas the Bi substituted samples strongly depend on the atmosphere in the measured temperature range. The highest values with $ZT_{870\text{K}} = 0.19$ (air) and $ZT_{870\text{K}} = 0.15$ (Ar) were achieved with $x = 0.20$.

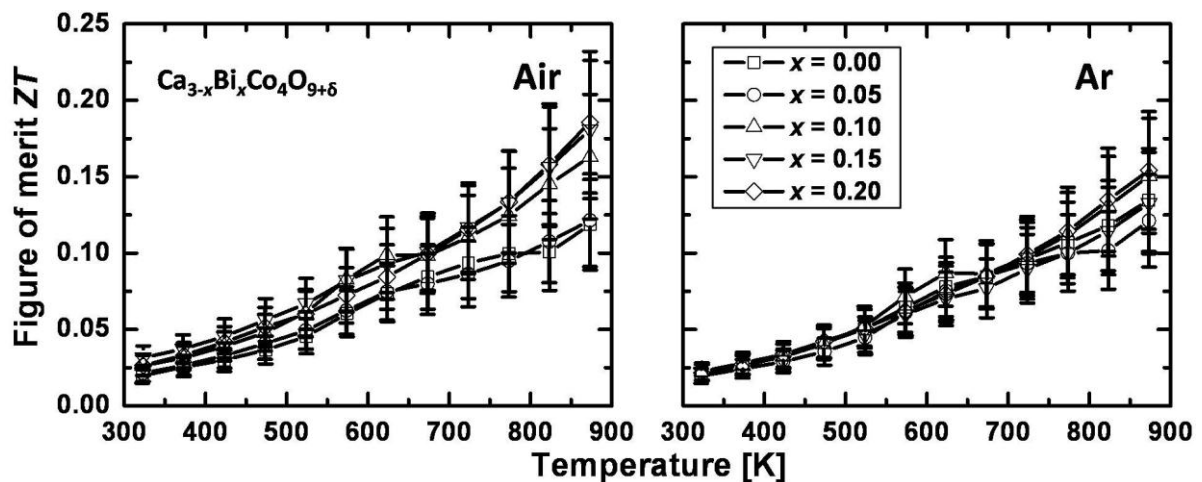


Figure 10: Figure of Merit of $\text{Ca}_{3-x}\text{Bi}_x\text{Co}_4\text{O}_{9+\delta}$ measured in (a) air and (b) argon atmosphere. A maximum relative error $\Delta(ZT) = \pm 25\%$ was determined by repeated measurements with identical samples.

National and international cooperation

Dr. Anton Rechsteiner, vonRoll casting

Jürg Hulliger, University Bern

Wulf Glatz, greenTEG

Christian Jooß, University of Goettingen

Conclusion and Outlook

All milestones of the first funding period were reached.

As the first step, the melting furnaces at vonRoll casting were identified as an appropriate location for the installation of thermoelectric generators. Measurements of the temperature boundary conditions over the course of an average production cycle were started and the lateral temperature profile on the top of the furnace cover was captured by an infrared camera. Evaluation of the data is in progress. Moreover, heat flux measurements are in preparation in order to be able to optimize the modules and to estimate the electrical generator output.

As a second step, based on a literature study and the assessment of existing technologies, ceramic materials were identified to be the most suitable materials under these conditions, because conventional materials are not resistant to temperatures higher than 200° C.

In addition, the use of modules containing toxic materials is dangerous as there is a risk of damage due to mechanical forces, for example during the installation of the gas burner. The application of materials requiring inert atmospheres is inappropriate as well. Furthermore, the operation in air is much cheaper and easier to realize and to guarantee.

Finally, misfit-layered cobaltates were synthesized using a simple and scalable synthesis method, which was optimized to provide reproducible results. In this first funding period we have shown that the ZT of oxide materials can be enhanced by changing the composition: On the one hand the thermal conductivity was lowered by about 40% by substitution with heavy elements like Bismuth. On the other hand, the electrical conductivity was improved by about 30 -50 % depending on the temperature due to an increase of the oxygen content. The Figure of Merit ZT could be improved from 0.12 ($x = 0.00$, both air and Ar) to 0.19 ($x = 0.20$, air) and 0.15 ($x = 0.20$, Ar) by modifying the Bi and the oxygen content, respectively. Moreover, our results reveal that the oxygen content is important for the thermoelectric properties of misfit-layered cobaltates.

When the evaluation of the boundary conditions is finished based on theoretical considerations, a matching material system, i.e. a combination of p- and n-type material with a good thermoelectric compatibility, will be chosen.

The approved synthesis routes will be adapted to produce further thermoelectric materials. A test module based on the synthesized thermoelectric materials will be built and tested and the efficiency will be further improved by optimization of the module geometry. The synthesis will be upscaled and demonstrator modules will be fabricated. Following principal laboratory tests installation at vonRoll casting and tests under real working conditions are planned.

References

- [1] Weidenkaff, A., Robert, R., Aguirre, M.H., Bocher, L., Lippert, T., S. Canulescu, *Renewable Energy*, 33 (2008) 342-347
- [2] Robert, R. Aguirre, M. H., Hug, P., Reller, A. and Weidenkaff, A., , *Acta Mat.*, 55 (2007) 4965-4972
- [3] Bocher L., Aguirre M.H., Robert R., Logvinovich D., Bakardjieva S., Hejtmanek J. and Weidenkaff, A., *Acta Mat.* 57 (2009) 5667-5680
- [4] Weidenkaff, A., Aguirre, M., Bocher, L., Trottmann, M., Tomes, P., and Robert, R., *J. Korean Cer. Soc.*, 47, (2010) 47-53
- [5] Moser, D., Karvonen, L., Populoh, S., Trottmann, M., Weidenkaff, A., *J. Solid State Sciences*10.1016/j.solidstatesciences.2011.10.001
- [6] Kittel, C. *Einführung in die Festkörperphysik*, 14th ed.; Oldenbourg, 2006, p. 176
- [7] Chaikin, P. & Beni, G. *Phys. Rev. B* 13, 647-651 (1976)
- [8] G. J. Snyder, Eric S. Toberer, *Nature Materials* 7 (2008) 105 - 114
- [9] I. Terasaki, Y. Sasago, K. Uchinokura, *Phys. Rev. B* 56 (1997) R12685
- [10] M. Shikano, R. Funahashi, *Appl. Phys. Lett.* 82 (2003) 1851
- [11] N.V. Nong, C.-J. Liu, M. Ohtaki, *J. Alloy. Compd.* 491 (2010) 53
- [12] Y. Liu, Y. Lin, L. Jiang, C.-W. Nan, Z. Shen, *J. Electroceram.* **21** (2007) 748
- [13] J. J. Shen, X. X. Liu, T. J. Zhu, X. B. Zhao, *J. Mater, Sci.* **44** (2009) 1889
- [14] W. Koshibae, K. Tsutsui, S. Maekawa, *Phys. Rev. B* **62** (2000) 6869

List of conference contributions and scientific publications in the 2011 funding period

- Moser, D.; Karvonen, L.; Populoh, S.; Trottmann, M.; Weidenkaff A., **Influence of the oxygen content on thermoelectric properties of $\text{Ca}_{3-x}\text{Bi}_x\text{Co}_4\text{O}_{9+\delta}$ system**, *Solid*

State Sciences (2011); corrected proofs accessible at
doi:10.1016/j.solidstatesciences.2011.10.001

- Moser, D.; Karvonen, L.; Populoh, **Thermoelectric properties and Oxygen Content of $\text{Ca}_{3-x}\text{Bi}_x\text{Co}_4\text{O}_9$ ($0.00 < x < 0.20$)**, 3e cycle seminar: "Synthesis and function of thermoelectric materials", Villars-sûr-Ollon, Switzerland (2011)
- Moser, D.; Karvonen, L.; Populoh, Weidenkaff A., **High-temperature thermoelectric properties and oxygen content of poly crystalline $\text{Ca}_{3-x}\text{Bi}_x\text{Co}_4\text{O}_{9+\delta}$** , "International Discussion Meeting on Thermoelectrics and related functional Materials", Helsinki, Finland (2011)